Preparation and Reactivity of Lepidocrocite under Simulated Feedwater Conditions

G. Bryce McGarvey*

Atomic Energy of Canada Limited, Chalk River Laboratories, Chalk River, Ontario, Canada K0J 1J0

K. Barrie Burnett and Derrek G. Owen

Atomic Energy of Canada Limited, Whiteshell Laboratories, Pinawa, Manitoba, Canada R0E 1L0

Lepidocrocite (γ-FeOOH), prepared using several different aging temperatures and aging times, possesses widely varying morphological and structural features. Mean particle dimensions and surface areas were all found to depend on the conditions of the synthesis. Studies of the aqueous reduction of several of the lepidocrocite samples to magnetite indicated that the initial steps in the dissolution−reprecipitation process were influenced by the crystallinity of the material. Results of the morphological studies and the transformation reaction studies are described within the context of corrosion-product generation and stability in secondary feedwater systems of pressurized heavy-water nuclear reactors.

Introduction

In CANDU (CANDU is a registered trademark of Atomic Energy of Canada Limited) generating stations, the secondary feedwater piping and the shells of the major feedwater heaters and steam generator components are constructed from carbon steel. When carbon steel corrodes, the final distribution of products will to a large extent reflect the environment that the metal was exposed to during the degradation process. Complex corrosion phenomena are encountered in aqueous environments due to changing redox conditions and levels of impurities. Despite operating with low impurity levels (<10 μg/kg of Cl^- and SO_4^{2-}), feedwater pH in the 9.5−10 range, and oxygen levels reduced to <10 μg/kg, by both mechanical deaeration and chemical scavenging with hydrazine (N_2H_4) (Brubaker and Geoffrey, 1988), carbon-steel corrosion is an ongoing issue because of its contribution to steam generator fouling. The principal corrosion products that have been identified in feed trains of nominally all-ferrous construction are magnetite (Fe_3O_4), hematite (α-Fe_2O_3), and lepidocrocite (γ-FeOOH); goethite (α-FeOOH) is a minor product (Sawicki and Brett, 1993).

The occurrence of γ-FeOOH as a more predominant product of aqueous-phase carbon-steel corrosion than α-FeOOH perhaps reflects the importance of reaction kinetics, rather than thermodynamics in transient processes such as these (Misawa et al., 1974). Although it is reported to be less thermodynamically stable than goethite (ΔG (lepidocrocite) = −470.5 kJ/mol and ΔG (goethite) = −496.2 kcal/mol) (Misawa, 1973), lepidocrocite can be synthesized by oxidizing Fe(II) ions in aqueous solution, and subsequently isolated in solid form.

In heavy-water-moderated CANDU reactors, the heat generated by nuclear-fission reactions is transferred to the heavy-water primary coolant as it circulates through the primary circuit (Figure 1). The heat is transferred through thin-walled tubing in the steam generators to the light water of the secondary circuit. The light water boils, producing steam to drive the turbine generator. The secondary circuit is completed by condensation of the exhaust steam from the turbine and recirculation of the condensate. Because the secondary feedwater circuit is a closed loop and the iron oxides that are generated as corrosion products are involatile, secondary-side fouling of steam generators in nuclear reactors is a serious issue for operating utilities (Turner and Godin, 1994). The principal concerns are two-fold: the possible reduction in heat-transfer efficiency from the primary water to the secondary water and formation of deposits on the tube surfaces that can concentrate aggressive impurities and create regions that are susceptible to underdeposit corrosion. Deposit samples removed from steam generators indicate that they are composed primarily of magnetite, with lesser quantities of hematite, but neither lepidocrocite nor goethite are observed. The reduced complexity of the iron oxide distribution in the steam generator deposits is a result of the effects of high temperature (>250 °C), heat flux, and the presence of hydrazine (N_2H_4), which favors the chemical reduction of the more highly oxidized α-Fe_2O_3 and γ-FeOOH phases. Evidently, conditions are also most favorable for the precipitation of Fe_3O_4 once the solubility limit for soluble iron species has been exceeded.

Variations in the distribution of corrosion products along the feed train as the temperature increases can be most readily attributed to (a) interconversion reactions between the phases or (b) preferential generation of one or more phases by different corrosion mechanisms in different sections of the feed train. Several interconversion reactions are possible between Fe_3O_4, α-Fe_2O_3, and γ-FeOOH. Under oxidizing conditions, γ-FeOOH is less thermodynamically stable than hematite, and under reducing conditions, both γ-FeOOH and α-Fe_2O_3 are less stable than Fe_3O_4. Lepidocrocite is therefore expected to transform to one of these phases, and its persistence at the higher-temperature sampling points

* Corresponding author. E-mail: mcgarveyb@aecl.ca. Telephone: (613)-584-8811, ext. 4870. Fax: (613)-584-9433.

S0888-5885(97)00582-4 CCC: $15.00 Published 1998 by the American Chemical Society
Published on Web 02/02/1998

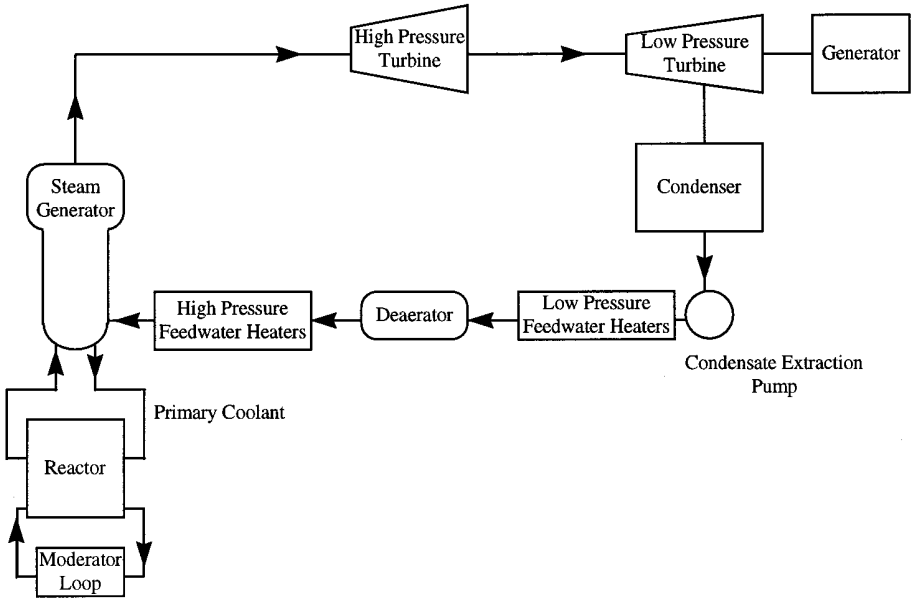

Figure 1. Schematic diagram of the primary and secondary circuits of a CANDU nuclear reactor.

of the feed train may reflect the kinetic limitations for the transformation reactions. The relationships between the three principal iron oxides under different conditions are shown in the following scheme:

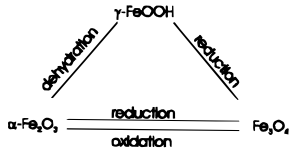

Among those most likely to occur in the feedwater are the reduction of γ-FeOOH or α-Fe_2O_3 to Fe_3O_4, the dehydration of γ-FeOOH to yield α-Fe_2O_3, or the oxidation of Fe_3O_4 to give α-Fe_2O_3. Many of the possible interconversion reactions of iron oxides have been studied, both in aqueous suspensions and in solid-state thermal reactions, particularly the hematite−magnetite transformations (McGarvey and Owen, 1996), and the decomposition of lepidocrocite to yield maghemite (γ-Fe_2O_3) (Gehring and Hofmeister, 1994), or hematite and goethite (Bechině et al., 1982).

The morphology of lepidocrocite is known to be very sensitive to the conditions leading to its formation. This phenomenon has been revealed under controlled laboratory conditions (Naono and Nakai, 1989) and also under plant conditions where powder X-ray diffraction (XRD) and scanning electron microscopic (SEM) evidence have been used to show the morphological variability. Figure 2a shows well-crystallized lepidocrocite deposits that were present on a corrosion-product transport filter. In several other cases, the breadth of the diffraction peaks indicated that the lepidocrocite was primarily composed of smaller particles that were less-crystalline than those shown in Figure 2b.

In this paper we describe a study of the synthesis and transformation of several lepidocrocite samples prepared with different morphological characteristics. The results are described primarily within the context of corrosion-product generation and transformation reactions that can occur in neutral and alkaline process water streams.

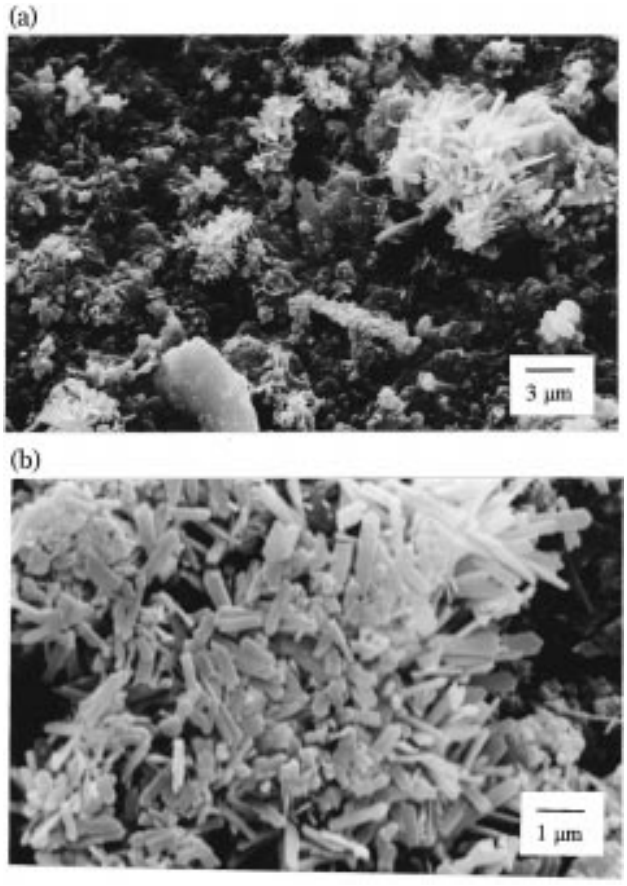

Figure 2. Electron micrographs of lepidocrocite samples removed from the secondary feedwater system of an operating CANDU nuclear reactor.

Experimental Section

Synthesis of Lepidocrocite. Subtly different procedures have been reported for the synthesis of lepidocrocite (Naono and Nakai, 1989; Ishikawa et al., 1993; Kumazawa et al., 1992). The following procedure for the γ-FeOOH synthesis is based on the work of Naono and Nakai (1989). Solutions of 1 mol/dm^3 NaOH and 0.24

Table 1. Summary of Conditions Used in the Synthesis of Lepidocrocite

run no.	aeration temp. (°C)	aging temp. (°C)	aging time (h)	Na_2HPO_4 present	residual PO_4^{3-} (μg/g)	type of base
1	10	50	2	yes	6.2	NaOH
2	10	50	24	yes	n.d.[a]	NaOH
3	10	50	1	yes	n.d.	NaOH
4	10	50	16	yes	n.d.	NaOH
5	35	50	16	no	n.m.[b]	morpholine
6	22	50	16	no	n.m.	morpholine
7	22	50	16	yes	4.3	morpholine
8	22	35	17	yes	3.7	NaOH
9	22	73	16	yes	75.0	NaOH

[a] n.d.: not detected. [b] n.m.: not measured.

mol/dm^3 HCl were prepared using previously boiled, distilled water, and the solutions were further purged for 30 min with ultra high purity N_2. Ferrous chloride ($FeCl_2 \cdot 4H_2O$, 0.48 mol) was dissolved in 300 cm^3 of the 0.24 mol/dm^3 HCl solution, vacuum-filtered through a medium porosity Hirsch funnel, diluted to 1000 dm^3 with 0.24 mol/dm^3 HCl, and transferred to a thermostatted polyethylene reaction flask.

The solution pH was adjusted to 7 with 1 mol/dm^3 NaOH and diluted to a final volume of 2000 cm^3 with boiled and purged distilled water. The flow of cooling (or heating) water was started, and once the desired temperature was achieved, air was bubbled through the solution at a rate of 500 dm^3/h for 3 h, during which time the pH dropped to 4. Anhydrous disodium hydrogen phosphate (0.035 mol) was added as a powder to the reaction mixture to suppress the nucleation of goethite. The temperature was raised to, and maintained at, the desired aging temperature for the prescribed period of time. The solution pH was maintained at 4 by adding aliquots of the base. The reaction mixture was cooled to room temperature and the solid phase allowed to separate for 72 h. Any adhering material was removed from the surface of the solution with ashless filter paper and the mixture was decanted. Any magnetite or maghemite that formed in the reaction was removed by magnetic separation. The precipitate was transferred to dialysis tubes which were sealed and placed in bottles that were equipped with a distilled water flow system that allowed for continuous replacement of the water. The conductivity of the water was monitored daily, and the procedure was terminated when the conductivity approached that of the distilled feedwater (approximately 30 days). Following the dialysis procedure, the washed γ-FeOOH was transferred to beakers and the suspension was allowed to evaporate to dryness. Table 1 lists the conditions that were investigated during the course of the study.

Characterization Methods. In order to determine the morphology and purity of the samples that were prepared, several physical and spectroscopic characterization methods were employed. Powder XRD patterns were recorded using CuKα radiation and a Rigaku Rotaflex diffractometer. Fourier transform infrared spectra were recorded from KBr disk specimens using a Bomem DA3 spectrometer in the absorbance mode. Scanning electron microscopy was carried out using either an ISI DS-130 scanning electron microscope or a JEOL 840-A scanning electron microscope. Transmission electron microscopy (TEM) of selected samples was carried out using a JEOL 200-B instrument. Samples were deposited onto copper TEM grids by dipping the grid into an aqueous suspension of the material and allowing it to dry. Nitrogen adsorption−desorption isotherms were measured using a volumetric glass system and surface areas were calculated using the BET theory.

Transformation Reactions. Selected lepidocrocite samples with different crystallinities were used in order to determine the effect of crystallite size and imperfections on the transformation to other products. Transformation reactions were carried out in 23 cm^3 autoclaves (Parr) equipped with poly(tetrafluoroethylene) liners. In a typical experiment, 0.1 g of iron oxide was placed in the autoclave with 15 cm^3 of water or aqueous solution. Depending on the requirements for the experiment, the samples were loaded and sealed either on the bench or in an anaerobic chamber. The autoclaves were placed in a preheated oven for 2−96 h and then cooled in air prior to opening. Most of the experiments were carried out at 150 °C; a smaller number were carried out at 100, 125, and 200 °C.

The hydrazine concentration selected for these experiments was 0.05 mol/dm^3 for 0.1-g aliquots of lepidocrocite and a total solution volume of 15 cm^3. A morpholine (tetrahydro-2*H*-1,4-oxazine) concentration of 50 mg/kg was used, except for some experiments in the absence of hydrazine, where a concentration of 100 mg/kg was used. In selected experiments, 1 mg/kg of Cu^{2+} was added to investigate the effect of a typical secondary-side metal ion on the reaction.

Results

Characterization of the Lepidocrocite Samples. The synthetic method yielded high-purity γ-FeOOH, provided that certain experimental conditions were maintained. The most critical variables for successful γ-FeOOH synthesis were the aeration temperature and the presence or absence of the sodium hydrogen phosphate. All syntheses that were performed with an aeration temperature in the range 10−22 °C with Na_2HPO_4 in the reaction mixture produced pure lepidocrocite samples as determined by infrared spectroscopy (well-resolved O−H stretching bands at 1155, 1022, and 748 cm^{-1} (Raman et al., 1991)) and powder XRD methods. Figure 3 shows two representative powder XRD profiles for γ-FeOOH samples prepared with different aging conditions. Note that there are significant differences in both the intensities and the breadth of the diffraction peaks, consistent with the higher degree of crystallinity for the material prepared with the longer aging time and higher temperature.

Omission of the sodium phosphate resulted in the formation of lepidocrocite that was contaminated with goethite (strong infrared bands at 798 and 893 cm^{-1}). The role of the phosphate anion is evidently to direct the nucleation process for the iron oxides toward the formation of lepidocrocite and suppress the formation of goethite. Detailed studies of the role of phosphate in directing the morphology of hematite by adsorbing on surface planes parallel to the *c*-axis leading to preferred growth directions have been reported by Ocaña et al. (1995). This mechanism is not likely to be responsible for directing γ-FeOOH formation since both lepidocrocite and goethite crystallize in acicular habits (Domingo et al., 1994). Instead, it can be speculated that phosphate ions influence the structure of the green rust intermediate and inhibit goethite nucleation.

The residual phosphate concentration on the iron oxide phase was minimized through the dialysis process;

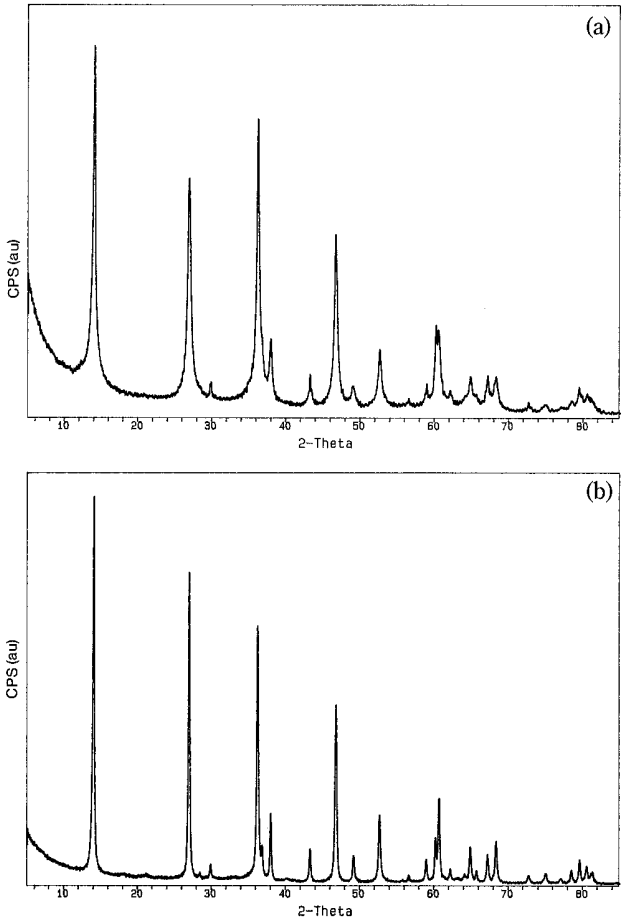

Figure 3. Powder X-ray diffraction patterns for two γ-FeOOH samples prepared using different reaction conditions: (a) aging time of 2 h at an aging temperature of 50 °C and (b) aging time of 16 h at an aging temperature of 73 °C.

Table 1 lists the measured concentration as determined using ion chromatography. Dialysis was found to be effective for reducing the concentration of phosphate below approximately 5 μg of PO_4^{3-}/g of γ-FeOOH. The exception was for run 9 in which the phosphate concentration was not reduced below 75 μg/g. There was no evidence for the formation of any iron phosphate phases; that is, they were below the XRD detection limit of ~1 wt % and no infrared bands attributable to phosphate ions could be assigned.

Lattice dimensions of the various γ-FeOOH samples were calculated using the standard relationships, and the mean crystallite dimensions were calculated using Scherrer's formula $L = K\lambda/\beta \cos\theta$ using $K = 0.9$ and $\beta = \Gamma - \Gamma_0$, where $\Gamma_0 = 0.08°$ (Klug and Alexander, 1974). The results are tabulated in Table 2. Crystallographic dimensions calculated for plant samples have been included in Table 2 to demonstrate the correspondence between synthetic lepidocrocite and that removed from the field.

In agreement with previous results (Naono and Nakai, 1989), the degree of crystallinity increased as the aging time was extended from 1 to 24 h. Figure 4a shows the increase in the mean crystallite dimensions as a function of aging time for samples that were prepared under otherwise identical conditions. Also included in Figure 4a is a plot of the change in the specific surface area of lepidocrocite as a function of aging time. Figure 4b shows the effect of aging temperature on the mean crystallite dimensions and the specific surface area of the particles. For both of these cases, the decrease in surface area that results from the longer aging time and higher aging temperature is attributed to the increased crystallinity of the materials. Since lepidocrocite does not possess an intrinsic internal porous network, the surface area changes are attributed directly to the particle size differences, that is, the

Table 2. Mean Crystallite Diameters for Lepidocrocite Prepared Using Different Synthetic Conditions and Retrieved from Operating Feedwater Systems

sample number	mean crystallite diameter (Å)		
	(020)	(120)	(031)
1	184	147	206
2	248	306	243
3	103	206	135
4	212	265	243
5	151	216	177
6	280	397	308
7	336	294	315
8	175	207	214
9	398	446	359
CEP-2	291	374	204
CEP-35	748	1047	674
5A-1	226	264	n.d.[a]
5A-10	336	534	360
5A-14	430	675	153

[a] n.d.: not determined.

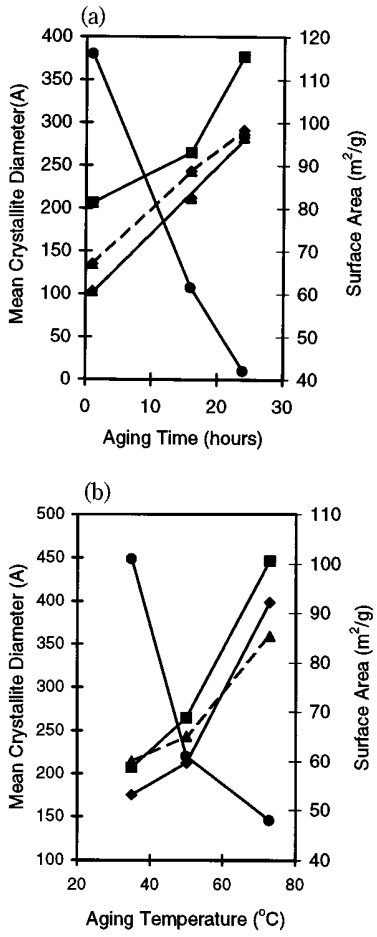

Figure 4. Calculated mean crystallite dimensions and measured surface areas for γ-FeOOH samples: (a) with an aging temperature of 50 °C for different periods of time and (b) for 16 h at different aging temperatures. Symbols: surface area (●). Mean crystallite dimensions: (120) plane (◆); (020) plane (■); (031) plane (▲).

external crystallite dimensions or the available interparticle surface. A comparison of the surface area changes with the changes in the mean crystallite dimensions confirms the relationship between particle morphology and surface area.

Selected samples were studied using transmission electron microscopy. Progressive increases in the crystallinity were observed as the aging time of the reaction was increased. Figure 5 shows representative lepidocrocite particles that were prepared with 1-h and 24-h aging times. The sample that had been aged for 1 h (Figure 5a) has a ragged structure, similar to that observed previously (Naono and Nakai, 1989). Extending the aging time allows crystal growth to proceed, and well-formed crystals such as those in Figure 5b result. The aging of the suspensions was done under constant stirring conditions and demonstrates that well-formed lepidocrocite crystals can form under agitated conditions. Figure 5c shows the structural differences between the two iron oxyhydroxides that were formed when morpholine was used as the base and no phosphate was added to the reaction mixture. The lepidocrocite particles are the larger lath-shaped crystals, while the fine, twinned crystals that resemble stars are goethite (Hsu and Marion, 1985). Both the infrared spectra and the powder XRD patterns revealed the presence of goethite in the product mixture.

Reduction of Lepidocrocite to Magnetite in Aqueous Hydrazine. Selected samples of lepidocrocite were subjected to reducing conditions in aqueous solution in order to assess the influence of preparation conditions, and hence morphology on the conversion reactions. The conditions for these static tests were designed to yield information for conservative simulations of the secondary feedwater. The majority of the experiments were carried out at 150 °C, with fewer experiments being done at 100 °C. Under the static test conditions at 150 °C, there was complete transformation of all lepidocrocite samples to magnetite after 4 h. With the experimental arrangement that was used, partial conversion of the lepidocrocite was detected only for 2-h reaction times. Shorter reaction times were not considered, because the autoclaves required a minimum of 1 h to achieve a stable reaction temperature. Scanning electron micrographs indicate that the magnetite crystals that form have a narrow particle-size distribution and are less than 100 nm in diameter (Figure 6). This is in contrast to the much larger magnetite particles (5−10 μm in diameter) that were generated from hematite in aqueous solutions of hydrazine (McGarvey and Owen, 1996).

There appears to be a correlation between the extent of conversion after a 2-h reaction and the aging conditions that were used in the preparation of the lepidocrocite. The lepidocrocite that was prepared with the shortest aging time and mildest conditions was completely converted to magnetite after a 2-h reaction time (Table 3). The other three samples that had aged for longer periods of time were more crystalline and had not reached 100% conversion after the same reaction time. This indicates that the morphology of chemically identical compounds does play some role in the interconversion reactions. It is reasonable to expect faster conversion for high surface area material, if the conversion proceeds by dissolution and reprecipitation.

Note that the presence of 1 mg/kg of Cu^{2+} in the reaction media inhibited the conversion of lepidocrocite

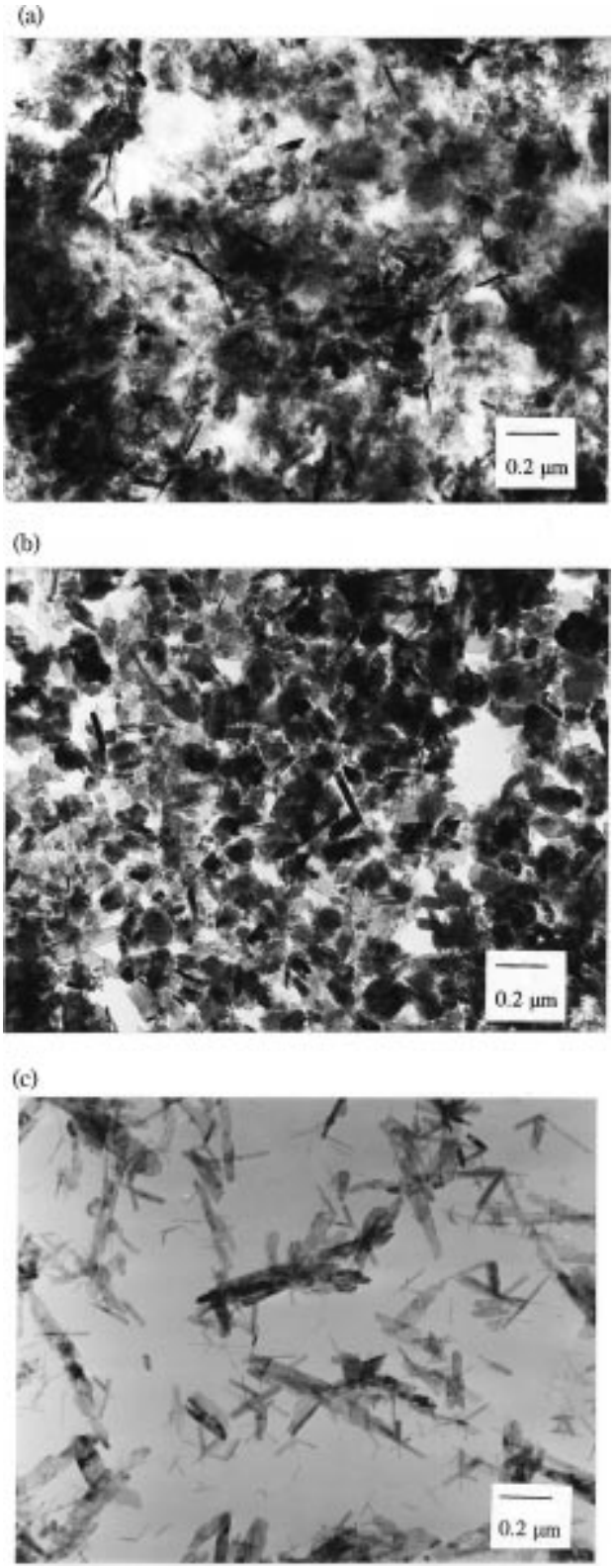

Figure 5. Transmission electron micrographs of γ-FeOOH samples prepared using different reaction conditions: (a) using an aging time of 1 h at 50 °C; (b) using an aging time of 24 h at 50 °C; (c) a mixture of γ-FeOOH and α-FeOOH obtained using an aging time of 16 h at 50 °C in the absence of phosphate ions. The lath-shaped particles are γ-FeOOH and the twinned needles are α-FeOOH.

(Table 3). Following the same 2-h reaction period, the conversion for each of the four lepidocrocite samples that were studied was significantly lower than in the case

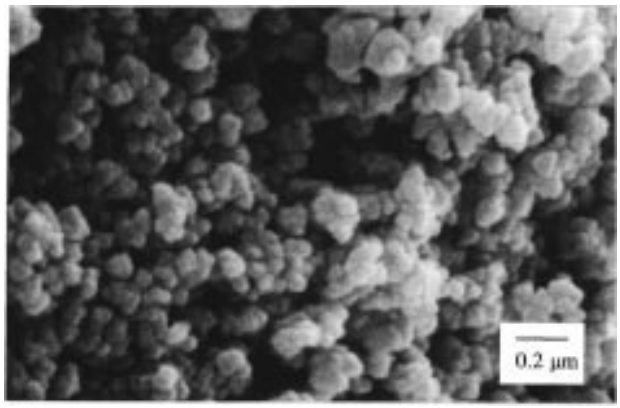

Figure 6. Scanning electron micrograph of the magnetite produced following the transformation of lepidocrocite at 150 °C for 24 h.

Table 3. Degree of Lepidocrocite Conversion for Several Samples after 2-h Reaction Time at 150 °C

lepidocrocite aging conditions	additives	conversion to magnetite (%)[a]	conversion to hematite (%)[b]
2 h at 50 °C	none	100	0
16 h at 50 °C	none	93	0
16 h at 35 °C	none	88	0
16 h at 73 °C	none	89	0
2 h at 50 °C	1 ppm of Cu^{2+}	85	0
16 h at 50 °C	1 ppm of Cu^{2+}	59	0
16 h at 35 °C	1 ppm of Cu^{2+}	80	0
16 h at 73 °C	1 ppm of Cu^{2+}	30	0

[a] Reaction in solution of 0.05 M hydrazine and 50 ppm of morpholine. [b] Reaction in solution of 50 ppm of morpholine.

where no secondary metal ion was added. We speculate that copper adsorption on the surface of the lepidocrocite retards the dissolution step of the transformation reaction. The inhibiting effect was minor, and complete conversion to magnetite was achieved after 4 h of reaction.

When lepidocrocite was heated in aqueous hydrazine at 100 °C, the reduction to magnetite was slower, as would be expected for the lower reaction temperature. Figure 7 shows a series of powder XRD patterns that were recorded for reaction times of 2, 4, 6, and 24 h. In Figure 7a, the lepidocrocite peaks dominate the pattern following a 2-h reaction period, although the development of the small diffraction peaks attributable to magnetite can be recognized. As the reaction time is increased to 4 and 6 h, the intensities of the magnetite peaks increase with a concomitant decrease in the lepidocrocite peak intensities. The diffraction pattern for the sample that was maintained at 100 °C for 24 h did not display any lepidocrocite peaks. This increased time for reaction is in contrast to the experiments at 150 °C, where the reaction was complete after 4 h for all studies of the different lepidocrocite samples.

Dehydration of Lepidocrocite in Aqueous Systems. A limited number of experiments were carried out to evaluate thermal effects in pure water and in 50 mg/kg morpholine solutions, in the absence of hydrazine. Lepidocrocite can undergo two different reactions in pure water: transformation to the more stable goethite phase and dehydration to hematite. In pure oxygenated water, there was no detectable conversion of the lepidocrocite at 150 °C after 96 h. When the reaction temperature was increased to 200 °C, complete dehydration to hematite occurred, but there was a significant induction period. Trace quantities of hematite were detected after 18 h, followed by completion of the reaction after 24 h.

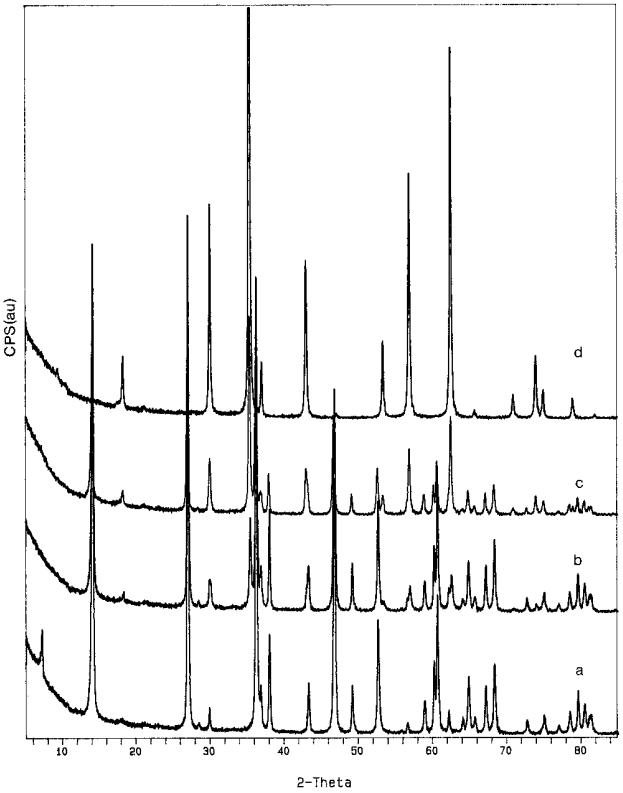

Figure 7. Powder X-ray diffraction patterns demonstrating the conversion of lepidocrocite to magnetite using a reaction temperature of 100 °C in 0.05 mol/kg of hydrazine: (a) 2-h reaction time; (b) 4-h reaction time; (c) 6-h reaction time; (d) 24-h reaction time.

Similarly, there was no detectable conversion of any of the lepidocrocite samples at 125 or 150 °C after 96 h. This was also the case for experiments at 150 °C in the presence of 1 mg/kg of Cu^{2+} (Table 3). As was observed in pure water, raising the temperature to 200 °C in morpholine did bring about the eventual dehydration of lepidocrocite, although 16−24 h were required for complete conversion. In the morpholine solution, a slightly greater degree of conversion was observed after 16 h than what had been observed in pure water after 18 h.

Discussion

Lepidocrocite Synthesis and Morphological Characterization. To help relate our experimental results to the behavior of lepidocrocite in feedwater systems, we have examined a number of corrosion-product specimens from various points in the secondary feedwater system of CANDU nuclear reactors (Bruce Nuclear Generating Station B, Units 5 and 8). The typical sampling points and approximate feedwater temperature at these locations are as follows: condensate extraction pump (35 °C) and the high-pressure feedwater heater (150 °C). Table 2 lists mean crystallite dimensions for synthetic lepidocrocite and also for lepidocrocite that was one component of a multicomponent distribution of corrosion products. The large degree of variability in the values reflects the difficulties in attempting to characterize and understand plant data where conditions can change significantly during the course of operation. In some cases, lepidocrocite was a

minor component of the mixture, while in others it was the dominant iron-containing phase. Nevertheless, it is apparent from the data in Table 2 that lepidocrocite prepared in this study is comparable in morphology to corrosion-product lepidocrocite and can be used with some confidence in laboratory studies to investigate events that occur in industrial settings.

Transformation Reactions of Lepidocrocite. Relatively few studies of the reduction of iron oxyhydroxides are reported in the literature. Blesa et al. (1986) have studied the reduction of akaganeite to magnetite in concentrated hydrazine solutions. On the basis of their results, a dissolution−reprecipitation process for lepidocrocite (eq 1) can be proposed.

$$12\gamma\text{-FeOOH(s)} + \text{N}_2\text{H}_4\text{(aq)} \rightarrow 4\text{Fe}_3\text{O}_4\text{(s)} + 8\text{H}_2\text{O} + \text{N}_2 \quad (1)$$

The initial step (eq 2) involves partial dissolution of the ferric oxyhydroxide, followed by reduction in hydrazine, to produce aqueous ferrous ions (eq 3). The ferrous ions adsorb on the surface of undissolved lepidocrocite particles, which drives the reaction to magnetite (eq 4)

$$\gamma\text{-FeOOH(s)} + \text{H}_2\text{O} \rightleftarrows \text{Fe}^{\text{III}}\text{(aq)} + 3\text{OH}^- \quad (2)$$

$$4\text{Fe}^{\text{III}}\text{(aq)} + \text{N}_2\text{H}_4 \rightarrow 4\text{Fe}^{\text{II}}\text{(aq)} + \text{N}_2 + 4\text{H}^+ \quad (3)$$

$$\text{Fe}^{\text{II}}\text{(aq)} + 2\gamma\text{-FeOOH(s)} \rightarrow \text{Fe}_3\text{O}_4\text{(s)} + 2\text{H}^+ \quad (4)$$

The involvement of ferrous ions produced by ferric ion reduction in hydrazine is consistent with previous studies of magnetite formation from lepidocrocite in solutions containing ferrous ions but no additional chemical-reducing agent (Tamaura et al., 1983). This study found that magnetite was produced when the pH of aqueous Fe(II) and γ-FeOOH mixtures was raised to 9 at 25 °C. Once again, the authors report that the reaction proceeds via a dissolution−reprecipitation process once the Fe(II) adsorption has occurred. The authors state that goethite was not converted to magnetite under the same conditions. Although the reasons were not discussed, it can be supposed that the structural differences between the two polymorphs, and the reported thermodynamic stability of goethite, are possible contributing factors. In addition, the O/OH sublattice in lepidocrocite is approximately cubic close-packed (ccp), and hence the low-temperature conversion to magnetite (also ccp) might reasonably be expected to be more facile than with goethite.

The present study confirms that magnetite forms from the lepidocrocite samples. The principal difference between the results here and those obtained by Blesa et al. (1986) for β-FeOOH is that the lepidocrocite appears to undergo slower initial dissolution than akaganeite. This may be due to differences in the solubilities of the two oxyhydroxide phases, or to the lower hydrazine concentration that was used in the present study.

If one considers the situation in the secondary feedwater system in an operating nuclear plant, the circuit time in the feed train (Figure 1) is rather short (<30 min) and the conditions are not isothermal. The results of this study suggest that under these conditions the probability for chemical transformation of suspended lepidocrocite to magnetite prior to transport to the steam generators is small. This is based on the fact that a reaction time of 4 h was required to ensure the complete conversion at 150 °C. These types of results are important pieces of information for station personnel who are responsible for chemistry control in the feedwater system.

Under the static conditions that were employed in this study, the dehydration of lepidocrocite to hematite did not proceed within the 96-h reaction time at temperatures up to 150 °C. Even at 200 °C, reaction times in excess of 16 h were required for this conversion, in marked contrast to previous reports that lepidocrocite converts to goethite and/or hematite in 2 h at 140 °C (Šubrt et al. 1980). Several explanations for this difference in behavior can be proposed. Lepidocrocite is believed to transform via a dissolution−reprecipitation process. It follows that lepidocrocite that is prepared with smaller particle sizes will dissolve more readily than larger crystals of the same material. The difference in the surface area (and hence particle size) of the lepidocrocite used by Šubrt et al. (1980) (~160 $m^2\ g^{-1}$) and that used here (40−100 $m^2\ g^{-1}$) may account for the different reaction times. The presence of a small amount of phosphate in our specimens is another possible factor. Phosphate binds strongly to most iron oxides (Persson et al., 1996) and is known to inhibit most iron oxide transformation reactions (Biber et al., 1994). In the present study, the effect of phosphate is expected to be minimal based on the fact that Biber et al. (1994) reported that inhibition is strongly pH-dependent and the reductive transformation experiments reported here were carried out in the pH-independent region (>9).

A final factor that can explain the differences in the observed reactivities is the purity of the samples. It has been reported that traces of goethite in a sample of lepidocrocite can direct the transformation toward the formation of goethite and subsequently hematite (Šubrt et al., 1980. Powder XRD and infrared spectroscopic data obtained in this study did not reveal the presence of goethite in the samples of lepidocrocite that were used for the transformation studies.

On the basis of the results of the experiments conducted in this study, suspended particles of lepidocrocite are not likely to transform to goethite or hematite under the conditions experienced in the feedwater systems. It should be emphasized, however, that these statements regarding the transformation of lepidocrocite are applicable only for suspended particulate. Corrosion products that adhere to pipe surfaces will be less susceptible to transport with the flowing water which is expected to provide sufficient time to undergo the dehydration or reduction reactions described above.

Acknowledgment

We thank D. A. Doern for recording the powder XRD patterns and R. Styles and F. Szostak for recording the TEM and SEM images. This work was funded by the AECL Underlying Chemistry Program and the CANDU Owners Group.

Literature Cited

Bechině, K.; Šubrt, J.; Hanslík, T.; Zapletal, V.; Tláskal, J.; Lipka, J.; Sedlák, B.; Rotter, M. Transformation of Synthetic γ-FeOOH (Lepidocrocite) in Aqueous Solutions of Ferrous Sulphate. *Z. Anorg. Allg. Chem.* **1982**, *489*, 186.

Biber, M. V.; dos Santos Alfonso, M.; Stumm, W. The Coordination Chemistry of Weathering: IV: Inhihition of the Dissolution of Oxide Minerals. *Geochim. Cosmochim. Acta* **1994**, *58*, 1999.

Blesa, M.; Miljalchik, M.; Villegas, M. Transformation of Akaganeite into Magnetite in Aqueous Hydrazine Suspensions. *React. Solids* **1986**, *2*, 85.

Brubaker, G. R.; Geoffrey, M. M. The Fate of Hydrazine in Pure, Deoxygenated, Aqueous Solutions at Elevated Temperatures and Pressures. *Ind. Eng. Chem. Res.* **1988**, *27*, 1149.

Domingo, C.; Rodriguez-Clemente, R.; Blesa, M. Morphological Properties of α-FeOOH, γ-FeOOH and Fe_3O_4 Obtained by Oxidation of Aqueous Fe(II) Solutions. *J. Colloid Interface Sci.* **1994**, *165*, 244.

Gehring, A. U.; Hofmeister, A. M. The Transformation of Lepidocrocite During Heating: A Magnetic and Spectroscopic Study. *Clay Clay Miner.* **1994**, *42*, 409.

Hsu, P. H.; Marion, G. The Solubility Product of Goethite. *Soil Sci.* **1985**, *140*, 344.

Ishikawa, T.; Nishimori, H.; Abe, I.; Kandori, K. Influence of the Adsorption of Citrate and Tartrate upon the Formation of γ-FeOOH Particles. *Colloids Surf. A* **1993**, *71*, 141.

Klug, H. P.; Alexander, E. A. *X-ray Diffraction Procedures for Polycrystalline and Amorphous Materials*; John Wiley and Sons: New York, 1974; p 656.

Kumazawa, H.; Inami, T.; Cho, H.-M.; Sada, A. Formation of Acicular Lepidocrocite Particles by Oxidation of Aqueous Suspensions of Ferrous Hydroxide. *Chem. Eng. Commun.* **1992**, *113*, 91.

McGarvey, G. B.; Owen, D. G. Copper(II) Oxide as a Morphology Directing Agent in the Hydrothermal Crystallization of Magnetite. *J. Mater. Sci.* **1996**, *31*, 49.

Misawa, T. The Thermodynamic Consideration for Fe-H_2O System at 25 °C. *Corros. Sci.* **1973**, *13*, 659.

Misawa, T.; Hashimoto K.; Shimodaira, S. The Mechanism of Formation of Iron Oxide and Oxyhydroxides in Aqueous Solutions at Room Temperature. *Corros. Sci.* **1974**, *14*, 131.

Naono, H.; Nakai, K. Thermal Decomposition of γ-FeOOH Fine Particles. *J. Colloid Interface Sci.* **1989**, *128*, 146.

Ocaña, M.; Rodriguez-Clemente, R.; Serna, C. J. Uniform Colloid Particles in Solution: Formation Mechanisms. *Adv. Mater.* **1995**, *7*, 212.

Persson, P.; Nilsson, N.; Sjoberg, S. Structure and Bonding of Orthophosphate Ions at the Iron Oxide-Aqueous Interface. *J. Colloid Interface Sci.* **1996**, *177*, 263.

Raman, A.; Kuban, B.; Razvan, A. The Application of Infrared Spectroscopy to the Study of Atmospheric Rust Systems-I. Standard Spectra and Illustrative Applications to Identify Rust Phases in Natural Atmospheric Corrosion Products. *Corros. Sci.* **1991**, *32*, 1295.

Sawicki, J. A.; Brett, M. E. Mössbauer Study of Corrosion Products From a CANDU Secondary System. *Nucl. Instrum. Methods Phys. Res.* **1993**, *B76*, 254.

Šubrt, J.; Hanslík, T.; Tláskal, J.; Zapletal, V.; Hanousek, F.; Hucl, M. Thermal Stability of Iron Oxide Hydroxide (Lepidocrocite) in Aqueous Suspensions. *Silikaty* **1980**, *24*, 255.

Tamaura, Y.; Ito, K.; Katsura, T. Transformation of γ-FeO(OH) to Fe_3O_4 by Adsorption of Iron (II) on γ-FeO(OH). *J. Chem. Soc., Dalton Trans.* **1983**, 189.

Turner, C. W.; Godin, M. Mechanisms of Magnetite Deposition in Pressurized Boiling and Non-Boiling Water. *Proceedings of the Steam Generator and Heat Exchanger Conference*; Canadian Nuclear Society: Toronto, Canada, 1994; p 7.111.

Received for review August 22, 1997
Revised manuscript received November 1, 1997
Accepted November 23, 1997

IE9705822